J. Phys. D: Appl. Phys. **31** (1998) 1100–1108. Printed in the UK PII: S0022-3727(98)89104-3

The effect of a large series resistance on the streamer-to-spark transition in dry air

Anders Larsson

Institute of High Voltage Research, Uppsala University, Husbyborg, S-752 28 Uppsala, Sweden

Received 11 November 1997

Abstract. The streamer-to-spark transition is an important sub-process of the flashover of high-voltage apparatus. In this paper an investigation of this transition in an electrode gap of the order of 1 cm in dry air with a non-uniform field distribution is presented. Parameters such as the gap distance, polarity of applied voltage and pressure were varied, but the study was concentrated upon the influence of a large series resistance (0–6 MΩ) in the discharge circuit (*inhibited discharges*). Mainly, the positive discharge was studied, but some results for negative applied voltages are also included. The main finding was that the presence of a large series resistance in the discharge circuit substantially prolonged the duration of the streamer-to-spark transition. The effect of the inhibiting series resistance seems to be that the disruptive discharge is delayed, but not prevented.

1. Introduction

The understanding of the streamer-to-spark transition is of importance for several areas of application, amongst them being the optimization of the design of outdoor high-voltage apparatus. The main objective of the study presented in this paper is to elucidate the influence of a large series resistance on the streamer-to-spark transition. Such discharges are termed *inhibited discharges*; that is the energy input into the discharge is limited by the presence of a large series resistance in the discharge circuit (Larsson 1997). Inhibited discharges occur frequently with outdoor high-voltage apparatus subjected to rain, the inhibiting ingredient being the water.

The streamer-to-spark transition in metallic electrode gaps of the order of 1 cm has been studied extensively over the years, but mainly in the following two arrangements (Marode 1983). The first consists of a needle-to-plane electrode configuration with a DC voltage being applied to the needle electrode. There is practically always a large resistance between the DC voltage source and the needle electrode. This series resistor serves two purposes. First, it protects the voltage source from the high current generated by the spark discharge and second, a well-chosen resistor value gives rise to a uniformly repetitive discharge in the electrode gap. Earlier, when the transient recorders had a lower sampling rate, the current oscillogram obtained was an average of many current impulses. Therefore a repetitive current impulse arrangement was needed. One disadvantage with this arrangement is that the gap voltage is not known, whilst another is that the earlier discharges will alter the characteristics of the air and significantly modify the discharge's behaviour (Hartmann and Gallimberti 1975).

The second arrangement consists of a DC voltage being applied across a large resistor, in series with a parallel plane electrode gap. The discharge was then initiated by UV irradiation of the cathode. In this case, no previous discharge process had altered the state of the air, but the gap voltage is not well defined during the streamer-to-spark transition.

Another ingenious arrangement consists of disconnecting the voltage source from the discharge gap by means of a capacitor, a crossbar arrangement (Cernak *et al* 1995). However, a disadvantage with such an arrangement is that the gap voltage is not kept constant during the streamer-to-spark transition.

In the light of the above-mentioned shortcomings, the following requirements for an experimental arrangement intended to clarify the influence of a large series resistance in the discharge circuit were indentified.

(i) Without a series resistor, the gap voltage should be constant during the streamer-to-spark transition. With a series resistor, the voltage across *the system* of the electrode gap plus series resistor should be constant.

(ii) No discharges should have occurred prior to the streamer-to-spark transition (that is, it should be a fresh gap discharge).

(iii) The gas composition and pressure should be controlled.

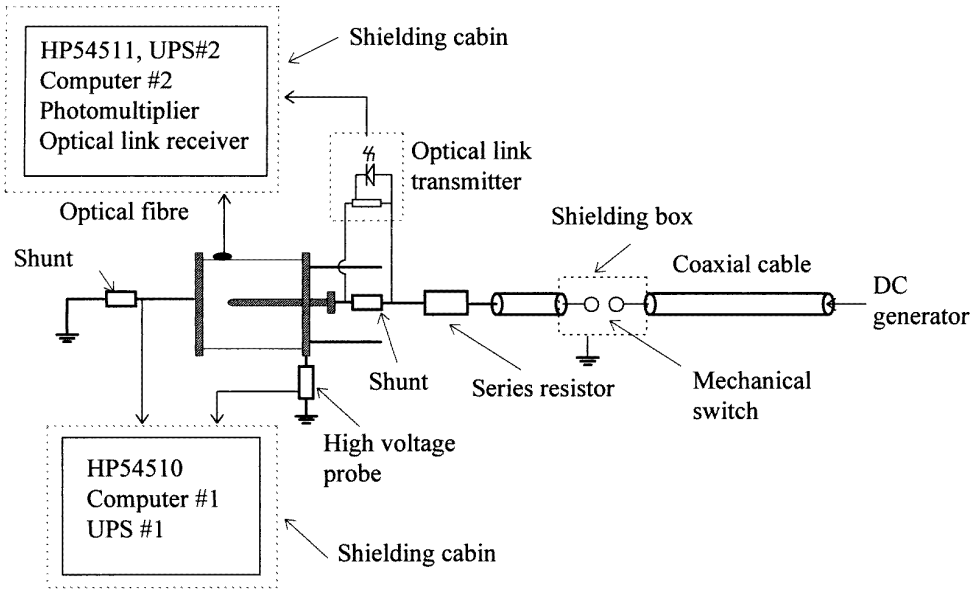

Figure 1. The experimental arrangement.

The measured parameters should be

(i) the streamer-to-spark transition current at both electrodes,
(ii) the gap voltage and
(iii) the optical radiation from the discharge.

The work is mainly concentrated upon the positive discharge, but some results for negative applied voltages are also included. Some early experimental results were discussed by Larsson *et al* (1996).

2. Experimental details

The electrode arrangement consisted of a rod-to-plane electrode configuration with a hemispherically tipped copper rod of 5 mm radius and a plane electrode made of brass. A protrusion (a short section of a Seirin acupuncture needle) was mounted on the tip of the rod electrode to achieve a strong enhancement of the electric field locally. The length and radius of curvature of the protrusion were 0.5 and 0.15 mm, respectively. The gap distance, measured from the tip of the protrusion to the plane electrode, was varied in the range 5–15 mm by means of a micrometer screw. The electrode spacing was enclosed by a plastic cylinder to control the humidity and the pressure of the gas, which was dry air (water content about 5 ppm). The pressure was varied between $0.5p_{amb}$ and p_{amb}, where p_{amb} is the ambient air pressure at the time of the measurement.

During the experiments the atmospheric conditions were as follows. The temperature was 20–21 °C and the atmospheric pressure p_{amb} was 1013–1020 hPa. These atmospheric data gave a relative air density δ in the range 1.00–1.01. The measured voltages were not adjusted to standard atmospheric conditions.

The experimental arrangement, including the voltage source and the measuring circuit, is shown in figure 1. The voltage across the gap was measured by using a 100 MΩ high-voltage probe (Tektronix P6015). The current was measured both at the earthed electrode and at the high-voltage electrode by using 0.1 Ω shunts, consisting of ten metallic film resistors (2 W each) connected in parallel, that had been designed in-house.

Three values of the series resistor have been used: zero, 600 Ω and 6 MΩ. An even larger value of the series resistance was not feasible since then it becomes of the same order of magnitude as the resistance of the high-voltage probe and thus the measuring circuit starts to have a significant influence on the discharge circuit.

The applied voltage was a fast-rising (nanoseconds) voltage impulse with a long decay time (hundreds of milliseconds) that was obtained by discharging a transmission line generator thorough the 100 MΩ high-voltage probe. The transmission line generator consisted of a 60 m long coaxial cable with a characteristic (wave) impedance of 50 Ω, which was charged by means of a DC voltage supply and was discharged by closing a mechanical switch.

The current impulse measured at the high-voltage electrode was transmitted by an optical link (Seniell 1000 FOL) and recorded by using a HP54111 transient recorder. The current at the earthed electrode and the gap voltage were recorded by using a HP54510 transient recorder. The sampling rate for both transient recorders was 1 Gsa s^{-1}. The data were stored on personal computers for subsequent processing and analysis. Furthermore, the equipment was placed in shielding cabins (Faraday cages) and disconnected from the mains with uninterruptable power supply (UPS) systems.

Optical emission from the discharge channel was measured with a photomultiplier (Hamamatsu R1477). The light was collected from the discharge via an optical fibre inserted into the electrode gap. This signal was

recorded by using the HP54111 transient recorder. The spectral sensitivity of the optical radiation measuring system was in the range 500–850 nm (Windmar 1994). The laboratory was darkened during the experiments to increase the sensitivity of the optical radiation measurements by reducing background noise. A thorough analysis of the measuring system has been made (Tang *et al* 1996, Larsson 1997) and the upper frequency limit of it was found to be 40 MHz.

The choice of trigger signal for the transient recorders was closely related to EMC considerations of the measuring circuit. Two different trigger systems were used. For the measurement of the voltage and the earthed electrode current, the disruptive discharge current was used as the trigger signal. As a trigger signal for the high-voltage electrode current measurement, the optical radiation associated with the disruptive discharge was used. The reasons for such an arrangement are as follows. Since the electronics of the optical link and the photomultipliers were very sensitive to electromagnetic interference from the discharge, no electrical trigger signal could be used as the trigger for the optical measurements. To avoid the interference from an electrical trigger, an optical fibre was used to detect the luminous event and trigger the current measurement equipment on the high-voltage side. Hence, the optical and electrical signal measurement circuits were isolated from each other. The trigger level was adjusted to allow the system to be trigged by the luminous event from the disruptive discharge. Apparently both the optical and the electrical signal measurements used the disruptive discharge as a trigger source. To record anything prior to the disruptive discharge when using it as the trigger source, a pre-trigger delay, typically of 3 μs, but sometimes of 8 μs, was used. However, the sampling rate was kept constant (1 Gsa s^{-1}). It should be noted that there was no exact synchronization between the two trigger systems, so the alignment of the currents in the oscillograms was achieved by overlapping the steep increase of the disruptive discharge current. The alignment error was of the order of 1 ns (just above the sampling rate).

In some cases, the triggering level for the light signal was set just above the noise level and, hence, the recorder was triggered by the first luminous event, namely the streamer discharge. No event was recorded with only a streamer discharge without a following streamer-to-spark transition.

3. General results

A typical oscillogram of the gap voltage for a disruptive discharge is shown in figure 2. The initial transients (caused by the capacitive current, reflections in the cable, electromagnetic noise and the shortcomings of the mechanical switch) occurring upon the application of the step voltage last for about 10 ms. The time between the application of the voltage impulse and the disruptive discharge was found to be 20–100 ms. The advantages of this particular impulse voltage shape are as follows. The initial transients do not interfere with the streamer-to-spark current measurement because of the late development of the

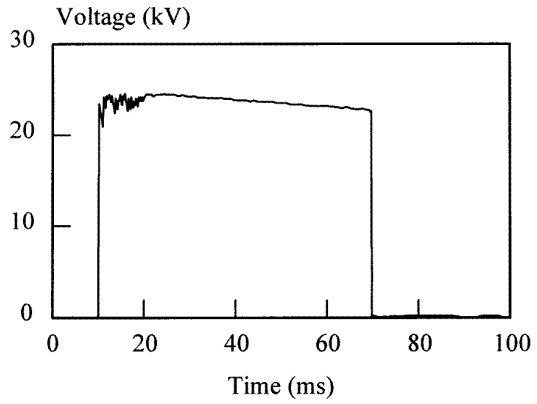

Figure 2. A typical oscillogram of the gap voltage impulse with a disruptive discharge.

disruptive discharge. Since the duration of the streamer-to-spark transition was found to be of the order of 1 μs or less (figure 3), the decay in the gap voltage can be neglected. Furthermore, the voltage was stable during the streamer-to-spark transition. This implies that the gap voltage was constant, measured and well defined during the transition and that no capacitive component arising from voltage variations across the gap was included in the current measurements. The long 'quiet period' between the application of the voltage and the discharge was attributed to the statistical time lag, namely the rate of detachment of free (seeding) electrons from negative oxygen ions (Berger and Hahn 1980).

Representative voltage and current oscillograms for the streamer-to-spark transition phase with a pre-trigger delay of 3 μs without a series resistor are shown in figure 3. In the current oscillograms, both the earth-side and the high-voltage-side currents are plotted. The voltage oscillograms show that the voltage was stable throughout the streamer-to-spark transition phase. No significant difference between the currents on the earth-side and on the high-voltage side were found during the first stage of the transition phase. During the final stage of the transition phase, however, some oscillations in the current on the high-voltage side were observed, especially with a negative voltage applied to the gap. These oscillations have a frequency of about 25 MHz and their origin has not been identified.

A closer look at the first part of the current impulse oscillogram reveals some characteristics of the first phase of the discharge (figure 4). Two regions, labelled 1 and 2, were recognized for positive applied voltages at the front of the current. The regions are less obvious for negative applied voltages and are therefore not indicated in figure 4 for that polarity. According to Marode (1975), who correlated current measurements to streak photographs, region 1 can be identified as the streamer propagation phase of the discharge and region 2 as the streamer's arrival at the plane electrode. However, Harrold (1974) interpreted region 2 as being a part of the streamer's propagation. The data collected in the present study are not suitable for a deeper discussion about the above-mentioned different interpretations of the regions 1 and 2. Lan *et al* (1997)

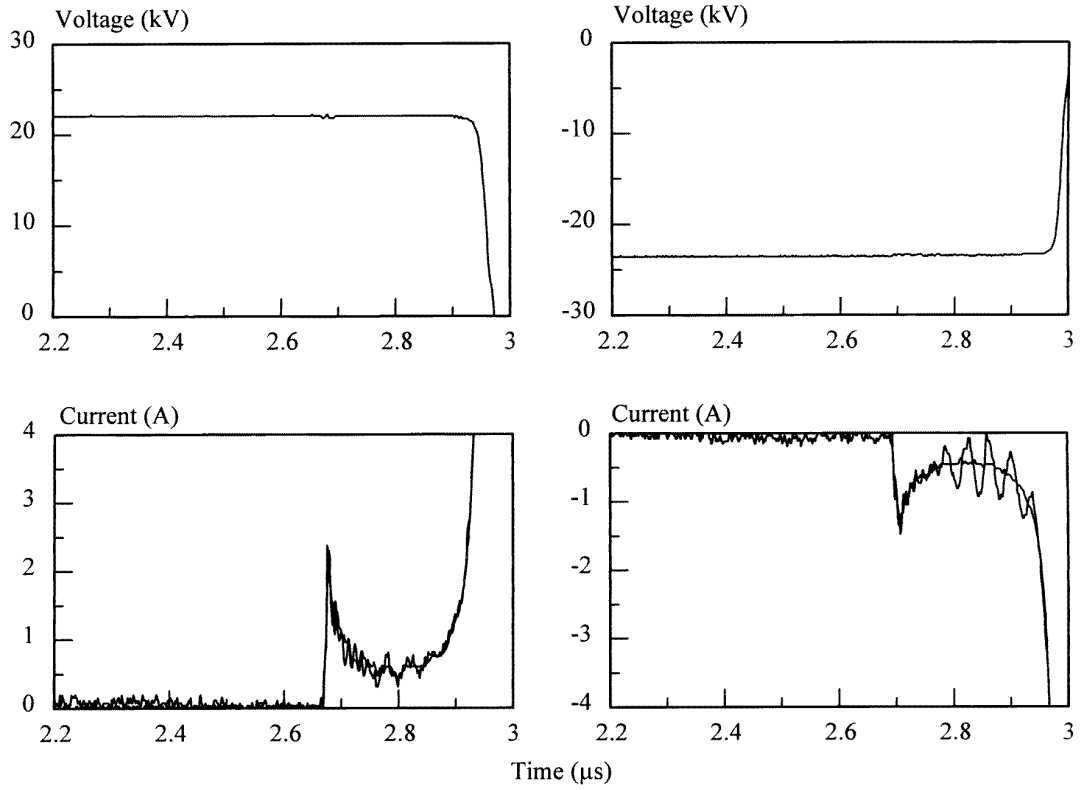

Figure 3. Typical voltage and current oscillograms for positive (left-hand side) and negative (right-hand side) applied voltage showing the constant voltage and the similarity between the currents during the discharge. Gap distance 10 mm, gas pressure p_{amb}; series resistor: none. Note that both the earth-side and high-voltage-side currents are plotted on the same oscillogram; the high-voltage current is the lighter line.

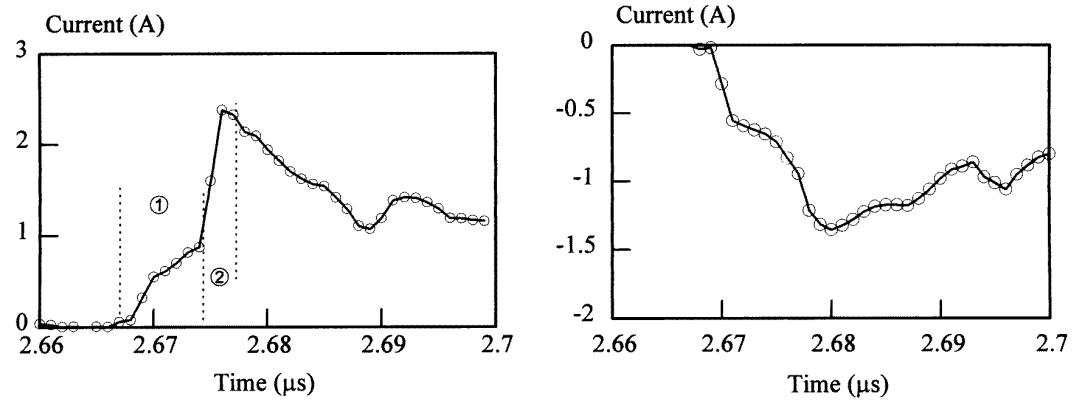

Figure 4. A close-up of the earth-side current oscillograms shown in figure 3. Each circle represents one sampled data point (1 ns per point). Region 1 is the streamer propagation phase of the discharge and region 2 is the streamer's arrival at the plane electrode.

interpreted region 1 as the streamer transit time and used this transit time to estimate the average streamer velocity. They found good agreement between these estimates and streamer velocity measurements using two optical fibres located at various positions along the gap. For the case of figure 4 (left-hand side), one obtains a velocity of about 1.4 Mm s^{-1} for the streamer, which is reasonable in the present mean background field strength (2.2 MV m^{-1}) (Kuffel and Zaengl 1984).

When studying the oscillograms for the streamer-to-spark transition current, it was recognized that a current measurement on only one electrode gives satisfactory information, since the currents on the earth side and on the high-voltage side were practically identical, except for the oscillations mentioned above. The current on the earth side of the gap was chosen to be measured because the high-voltage-side current measurement system was more sensitive to electromagnetic interference. Hence, in the

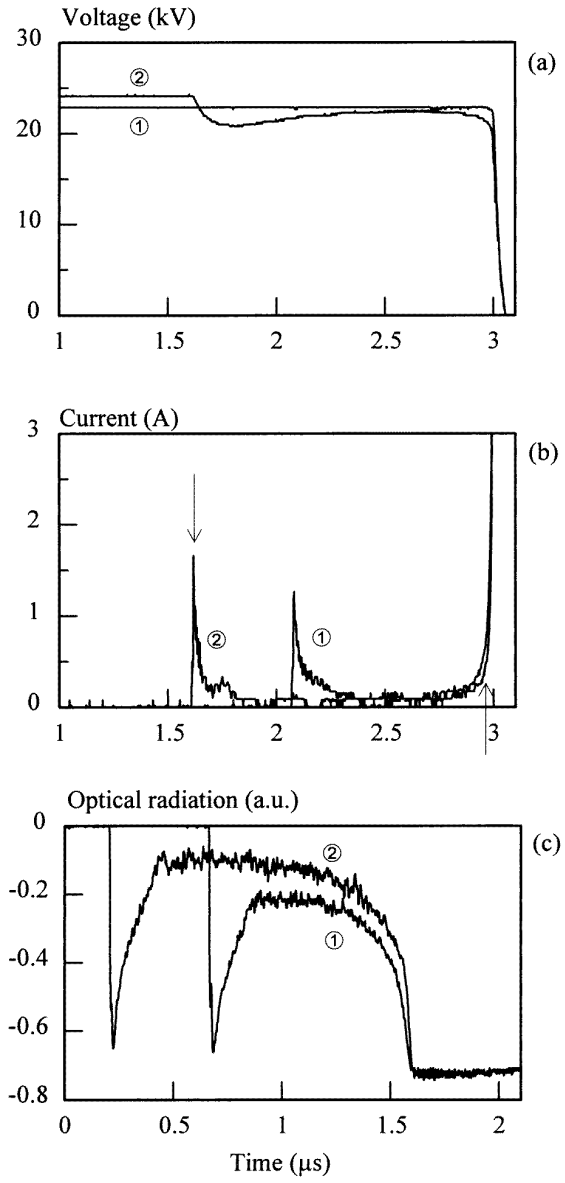

Figure 5. Illustrative voltage (a), current (b) and optical radiation (c) oscillograms. 1, without a series resistor; and 2, with a resistor of 6 MΩ. The lighter line is for the 6 MΩ resistor. Gap distance 10 mm and gas pressure p_{amb}. The difference between the time frames is the result of the use of different triggering signals. For the current curve 2, the starting and ending points of the streamer-to-spark transition are indicated by arrows (see the text).

second series of experiments, only the earth-side current was measured.

Illustrative voltage, current and optical radiation oscillograms of the streamer-to-spark transition phase without and with a series resistor, the value of which was 6 MΩ, and with a pre-trigger delay of 3 μs are shown in figure 5. With the series resistor, the gap voltage clearly decreased during the initial discharge phase, then it slowly recovered towards the voltage level it had had prior to the initiation of the discharge. The effect of the series resistance is explained as follows. Prior to the streamer-to-spark transition, the resistor had no influence on the gap voltage. When the discharge started, the capacitive energy stored in the gap was partly released and the gap voltage was reduced. To compensate for this reduction in voltage, the gap capacitance needed to be recharged by the generator. Without any series resistance, the generator charging current was only dependent on the characteristic impedance of the generator cable (50 Ω) and, hence, the recharging was quick and no drop in the gap voltage was observed. However, with a large series resistance, the charging current was limited and therefore a drop in the gap voltage was measured. After the initial peak in the streamer-to-spark transition current, the current remained low (but finite) and the gap voltage started to recover.

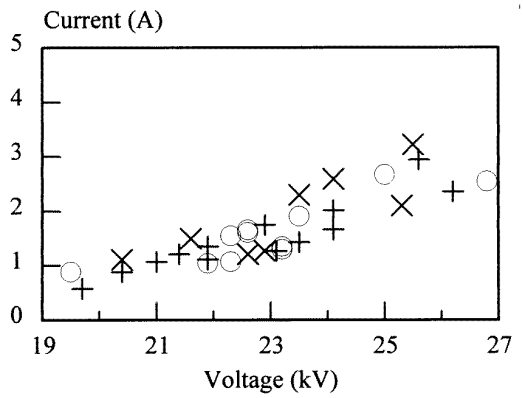

Figure 6. The relationship between the gap voltage and the peak streamer discharge current for various values of the series resistance. Gap distance 10 mm, gas pressure p_{amb}; ×,0 Ω; ○, 600 Ω; and +, 6 MΩ.

The gap capacitance can be estimated from the reduction in the gap voltage by using the definition $C = \Delta Q/\Delta U$. ΔQ is the charge injected into the gap during the discharge; it can be calculated by integrating the measured current. ΔU is the voltage change brought about by the injection of ΔQ. Such an estimation of the capacitance gives the rough value of $C = 15$ pF. The estimate should be compared with the value of 16 pF achieved from electrostatic field calculations (Tang *et al* 1996). A further observation of interest was that the minimum voltage required for the occurrence of a disruptive discharge was not influenced by the magnitude of the series resistance.

The primary parameters measured were the gap voltage and the streamer-to-spark transition current. Figure 6 shows the relationship between the gap voltage and the peak streamer current (region 2 in figure 4) for various magnitudes of the series resistance. In the case of a series resistor, the gap voltage immediately prior to the first discharge event has been chosen; that is, the voltage amplitude before the voltage reduction caused by the initial discharge current (see figures 5(a) and (b)). The peak transition current exhibits an increase with the gap voltage, but no difference was found for various resistances. However, one should carefully consider the sampling rate when using peak current amplitudes (as is evident from figure 4). A sampling rate which is too low may lead one to miss the peak value and the current oscillogram will not give a correct value for the peak amplitude.

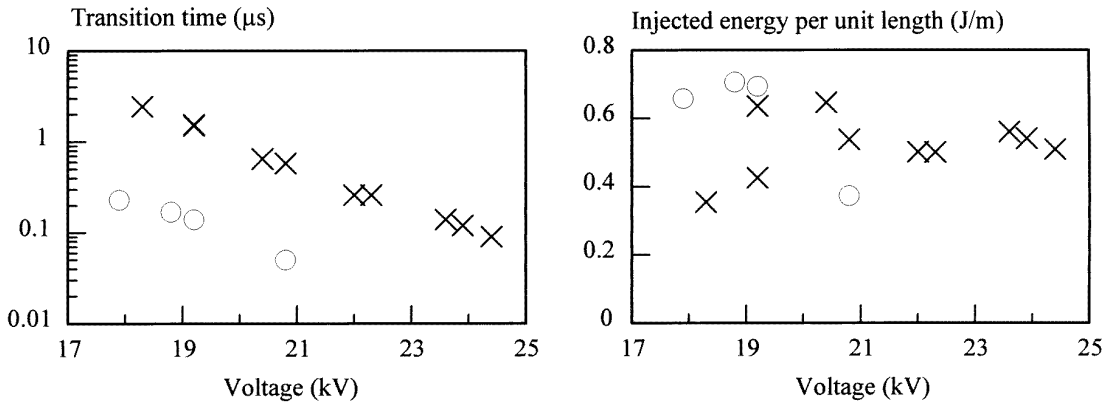

Figure 7. The dependence upon the gas pressure. Positive polarity, gap distance 10 mm, no series resistor; ×, p_{amb}; and ○, 0.75 p_{amb}.

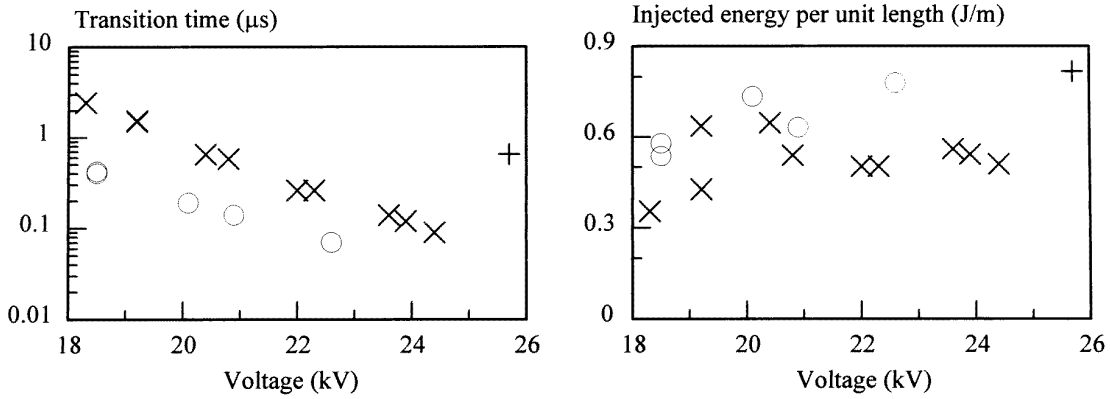

Figure 8. The dependence upon the gap distance. Positive polarity, pressure p_{amb}, no series resistor; ○, 8 mm; ×, 10 mm; and +, 12 mm.

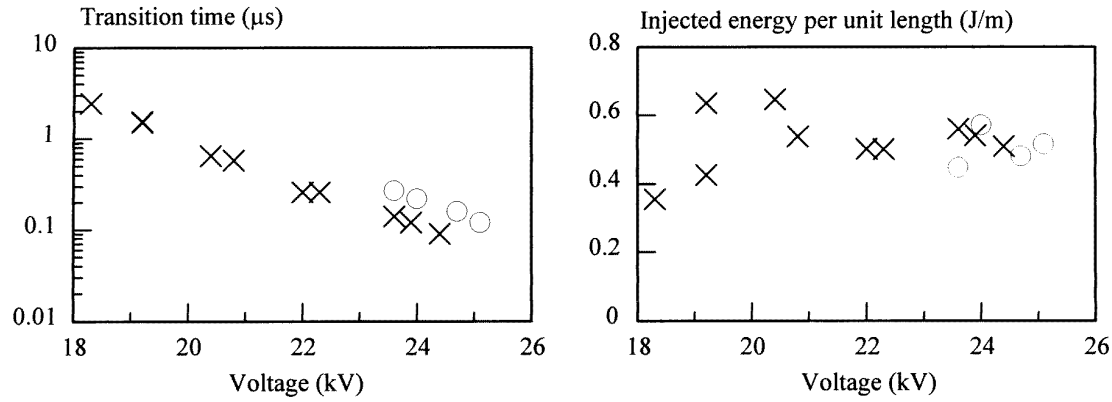

Figure 9. The dependence upon the polarity of the applied voltage. Gap distance 10 mm and pressure p_{amb}, no series resistor; ×, positive; and ○, negative.

4. The injected energy and the transition time

The analysis presented in this section is concentrated upon two parameters: the energy injected into the discharge channel and the streamer-to-spark transition time. The term 'transition time' is assigned to the time elapsing between the start and the end of the streamer-to-spark transition current, indicated by the arrows in figure 5. The starting point is the peak of the streamer current and the ending point is the point of inflection of the current curve. This rough definition was sufficiently accurate since the transition time was found to be at least a few hundred nanoseconds, which is one or two orders of magnitude greater than the rise time of the disruptive discharge current impulse. The injected energy was calculated from the integration of the measured input power (namely the product of the measured current

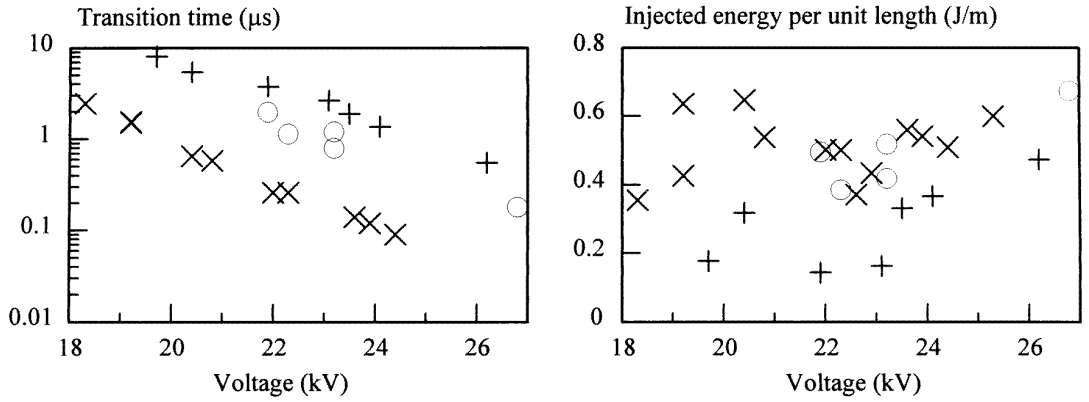

Figure 10. The dependence upon the magnitude of the series resistance. Positive polarity, gap distance 10 mm and pressure p_{amb}; ×, 0 Ω; ○, 600 Ω; and +, 6 MΩ.

and the measured gap voltage) over the transition time. In figures 7–10, the injected energy is normalized to the gap length. Unless otherwise stated, the conditions for the measurements were that the polarity of the applied voltage was positive, the gap distance was 10 mm, the pressure was p_{amb} and no series resistor was used.

Figure 7 illustrates the influence of the air pressure for a positive applied voltage. The amount of energy injected into the gap during the streamer-to-spark transition exhibited no air pressure dependence. However, for a given gap voltage, a lower pressure resulted in a shorter transition time. For a pressure lower than $0.75p_{amb}$, the transition time was too short for the streamer-to-spark transition current to be identified in the oscillograms.

Figure 8 indicates the influence of the electrode gap spacing for a positive applied voltage. For a given gap voltage, shorter transition times were observed in shorter gaps. For a gap distance shorter than 8 mm, the transition time was too short for the streamer-to-spark transition current to be identified in the oscillograms. The pattern of the current oscillogram was changed by increasing the gap length to 12 mm. Figure 11 gives an example for a gap length of 15 mm, for which a second peak in the current is observed. Only one peak in the current was observed for all cases with gap lengths of 8 and 10 mm. Except for one cases two peaks in the current were observed for all cases, with gap lengths of 12 and 15 mm. Only the cases with one peak are presented in figure 8, among which the single case of a 12 mm gap with only one peak is included. The 'multiple-peak' cases were not further investigated, but a report of the existence of such events has been published earlier (Suzuki 1971).

The plots for a negative applied voltage are similar to those for a positive applied voltage given in figures 7 and 8, whereas figure 9 indicates the difference caused by the polarity of the gap voltage. The same amount of injected energy was needed in both cases, but the transition time was slightly longer for a negative polarity.

Figure 10 displays the influence of an inhibiting series resistor. The transition time increased with increasing series resistance. Thus, the series resistance tends to delay the disruptive discharge.

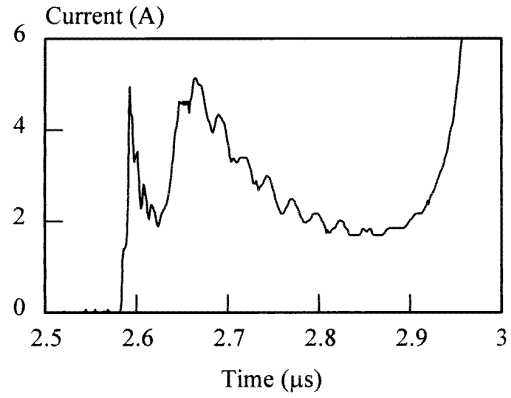

Figure 11. A current oscillogram with two peaks. Positive polarity, applied voltage 31 kV, gap distance 15 mm and pressure p_{amb}, no series resistor.

The main finding from figures 7–10 is that the transition time was strongly (exponentially) dependent on the gap voltage. The transition time exhibited a broad variation of magnitude, ranging from nanoseconds up to about 10 μs. In the literature, one can find reports of even longer transition times—hundreds of microseconds (Suzuki 1971, Lan and Scuka 1997). A further observation was that the energy injected was independent of the transition time. Figure 12 shows two current oscillograms with different streamer-to-spark transition times, but with the same energy having been injected. With a lower gap voltage, the peak of the streamer-to-spark transition current was smaller and the transition time was longer.

To state anything definite about the variation of the injected energy is difficult. Figures 7–10 indicate that the injected energy might be independent of the gas pressure and the polarity of the applied voltage and that there is a tendency for there to be a lower energy for shorter gap lengths and larger series resistances, but any conclusive statements are premature because of the limited amount of data points and the considerable scatter in the data. Anyhow, the amount of injected energy is, at most, weakly dependent upon the parameters, considering the range in which the parameters were varied.

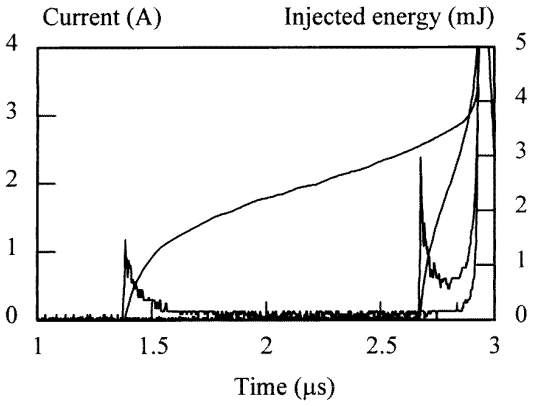

Figure 12. Two current oscillograms with different streamer-to-spark transition times together with corresponding injected energies (lighter lines). The gap voltage was 22 kV for the event with the short transition time and 19 kV for that with a long transition time.

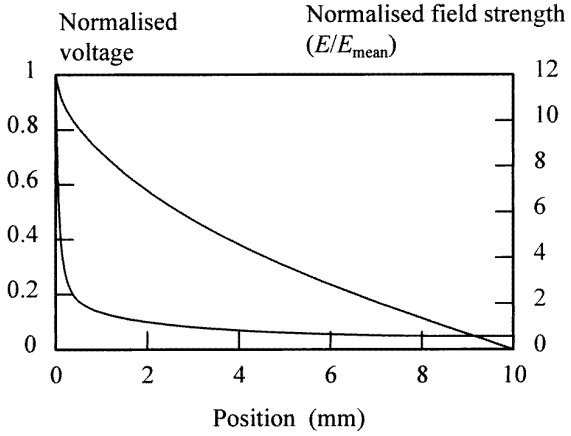

Figure 13. The potential and electric field distributions along the centre line for a gap length of 10 mm. The gap voltage was set to 1 V and the electric field strength is normalized with respect to the mean field strength in the gap.

5. Discussion

The potential and electric field distributions along the centre line in the electrode gap for a gap length of 10 mm are shown in figure 13. The calculations were performed using the charge simulation method (Ace 1996) and they are used in the estimation of the minimum streamer inception voltage, see below.

The minimum voltage required for the initiation of a streamer, the streamer inception voltage, can be estimated in the following way. A free (seeding) electron is accelerated in the electric field and the repeated ionizations of the air molecules cause an electron avalanche. The multiplication of the number of electrons is given by

$$N_e(x) = \exp\left(\int_0^x (\alpha - \eta)\,\mathrm{d}x'\right) \qquad (1)$$

were $N_e(x)$ is the number of electrons at the avalanche tip and α and η are the ionization and attachment coefficients, respectively. The integration path should be along an electric field line. It has been experimentally shown by Raether (1964) that, if an electron avalanche grows to about 10^8 electrons, the space charge in the avalanche tip creates an electric field that significantly adds to the background electric field distribution in the vicinity of its tip and the avalanche-to-streamer transition takes place. The coefficients α and η are strongly dependent on the electric field strength and are often expressed as a relation between reduced quantities, for example $\alpha/n = f(E/n)$, where n is the density of the neutral species in the gas. The use of analytical approximations of the function f is no more reliable than direct specification of the dependence of α/n on E/n on the basis of existing experimental data (Lagarkov and Rutkevich 1993). If one calculates the avalanche charge according to equation (1) along the field line in figure 13 using ionization and attachment data from Badaloni and Gallimberti (1972), an applied voltage of 16 kV gives rise to an avalanche of the critical size. This is the minimum voltage necessary for the inception and one requires that there is a seeding electron in exactly the correct position. Thus, the actual inception voltage is expected to be slightly higher. The experiments give a minimum voltage for the disruptive discharge of 18 kV. 16 kV applied to a 10 mm gap gives a mean electric field strength of 1.6 MV m^{-1}. Since the mean electric field strength at the minimum streamer inception voltage is greater by far than 450 kV m^{-1}, which is the minimum field for stable propagation of a streamer (Allen and Ghaffar 1993), the implication is that, once a streamer has been initiated, the streamer bridges the gap and initiates the streamer-to-spark transition. Even if one takes into account the reduction of the gap voltage when one has the 6 MΩ series resistor in the discharge circuit (figure 5), the field strength is still greater than the minimum field for stable propagation of a streamer.

Generally, the bridging of an electrode gap by a streamer is not necessarily followed by a spark discharge—as was first reported by Andersson (1958a, b)—but the conditions of the experimental arrangement presented in this paper (the electrode configuration and voltage source) apparently made the streamer-to-spark transition inevitable since no streamer discharge without a following spark discharge was observed. Furthermore, Marode *et al* (1979) and Windmar (1994) reported, both experimentally and theoretically, that, if the peak streamer current is greater than 0.1 A, the spark discharge will occur, otherwise it will not, whereas figure 6 shows currents of the order of 1 A.

The observations that no streamer discharge occurred without a following streamer-to-spark transition and that the minimum voltage at which a disruptive discharge occurred was not dependent on the magnitude of the series resistance indicate that the series resistance did not influence the value of the minimum streamer inception voltage. This and the observation that the streamer-to-spark transition time increased substantially with the series resistance suggest that the series resistance did not prevent the occurrence of a disruptive discharge, but only delayed it. The construction of the voltage source (a transmission line generator) gave a continuous feed of the discharge current, even though it

was provided through the inhibiting series resistor, which maintained the gap voltage and thus made the streamer-to-spark transition inevitable. However, in general, the relationship between the minimum voltage necessary for a disruptive discharge and the magnitude of the series resistance is dependent upon the shape of the applied voltage. Szpor *et al* (1978) subjected 1 cm gaps to 1.2/5 and 1.2/50 μs voltage impulses and found that the disruptive discharge voltage increased with the series resistance (in the range 0–100 kΩ) and that the increase was more pronounced for the impulse with the shorter tail.

The spark formation is believed to follow the mechanism outlined by Rogoff (1972) and further by Marode *et al* (1979) and Sigmond (1984), whereby the main process that leads to the final breakdown of the gap is mainly attributed to a gradual increase of the reduced field, E/n, through a decrease of the gas density n in the streamer channel, caused by a weak expansion shock set up by the heat deposited by the streamer current. When the reduced field is sufficiently increased, the ionization starts to dominate over the attachment and the spark is formed. A discharge development in which 'potential waves of ionization' are travelling back and forth in the streamer channel, as described by Loeb (1965) and Suzuki (1971), is not believed to be applicable to the results presented in this paper. This is because the 'complex' cases, such as that shown in figure 11, are excluded from the analysis; solely the cases with a straightforward streamer-to-spark transition consisting of only one peak in the current–light oscillograms (for example, see figure 5) were included.

The observation that the energy injected into the streamer channel prior to the spark discharge was independent of the streamer-to-spark transition time (for example, see figure 12) is consistent with the hypothesis that the heat deposited in the streamer channel by the streamer current necessary to increase the reduced field to the critical value is constant; that is, that the energy input is the important parameter. This hypothesis was neither verified nor falsified, for various series resistances, by the energy plots of figures 7–10 because of the limited amount of data points and the considerable scatter in the data.

6. Conclusions

The conclusions of the experimental investigation presented in this paper can be summarized in the following three items, which are valid for the particular experimental arrangement and parameter settings used.

(i) The magnitude of the series resistance is found not to influence the streamer inception voltage, the peak streamer current and the voltage needed to achieve that the streamer bridges the electrode gap.

(ii) The main influence of the presence of a large series resistance in the discharge circuit is that the streamer-to-spark transition time is substantially prolonged. The introduction of a 6 MΩ series resistance increases the transition time by one order of magnitude.

(iii) The energy injected into the gap during the streamer-to-spark transition is, at most, weakly dependent on the polarity of the applied voltage, the gap distance, the gas pressure and whether or not a large series resistance is present in the discharge circuit.

Or, in a few words, the effect of the inhibiting series resistance seems to be that the disruptive discharge is delayed, but not prevented.

Acknowledgments

The author would like to thank Professor Viktor Scuka for his continuous interest and support of this work and Professor Ivo Gallimberti for fruitful discussions. The experimental support from Dr Hong Tang is also greatly acknowledged.

References

Ace 1996 ABB common platform for field analysis and simulation–User Manual, ABB Corporate Research Internal Report (Västerås)

Allen N L and Ghaffar A 1993 *8th Int. Symp. on High-Voltage Engineering (Yokohama)* paper 40.02

Andersson N E 1958a *Ark. Fys.* **13** 399

——1958b *Ark. Fys.* **13** 441

Badaloni S and Gallimberti I 1972 Padua University Report UPee 72/05

Berger G and Hahn R 1980 *IEE Conf. Publ.* **189** 195

Cernak M, van Veldhuizen E M, Morava I and Rutgers W R 1995 *J. Phys. D: Appl. Phys.* **28** 1126

Harrold R T 1974 Annual Report CEIDP, NAS-NRC p 123

Hartmann G and Gallimberti I 1975 *J. Phys. D: Appl. Phys.* **8** 670

Kuffel E and Zaengl W S 1984 *High Voltage Engineering* (Oxford: Pergamon) p 373

Lagarkov A N and Rutkevich I M 1993 *Ionisation Waves in Electrical Breakdown of Gases* (Berlin: Springer)

Lan G, Cooray V, Thottappillil R and Scuka V 1997 *Proc. 1997 IEEE Conf. on Electrical Insulators and Dielectric Phenomena (Minnesota)* pp 587–90

Lan G and Scuka V 1997 *Proc. 10th Int. Symp. on High-Voltage Engineering (Montréal)* paper 3045

Larsson A 1997 *Inhibited Electrical Discharges in Air* (Stockholm: Almqvist & Wiksell)

Larsson A, Tang H and Scuka V 1996 *Proc. Nordic Insulation Symp.* (Bergen) pp 99–106

Loeb L B 1965 *Science* **148** 1417

Marode E 1975 *J. Appl. Phys.* **46** 2005

——1983 *Electical Breakdown and Discharges in Gases* ed E E Kunhardt and L H Luessen (New York: Plenum)

Marode E, Bastien F and Bakker M 1979 *J. Appl. Phys.* **50** 140

Raether H 1964 *Electron Avalanches and Breakdown in Gases* (London: Butterworth)

Rogoff G L 1972 *Phys. Fluids* **15** 1931

Sigmond R S 1984 *J. Appl. Phys.* **56** 1355

Suzuki T 1971 *J. Appl. Phys.* **42** 3766

Szpor S, Boryn H and Beroual A 1978 *Archiwum Elektrotechniki* **27** 483

Tang H, Larsson A and Scuka V 1996 *Proc. Nordic Insulation Symp.* (Bergen) pp 169–76

Windmar D 1994 *Water Drop Initiated Discharges in Air* (Stockholm: Almqvist & Wiksell)